Statetostate rotational energytransfer measurements in the v2=1 state of ammonia by infrared–infrared double resonance

Bernd Abel, Stephen L. Coy, Jody J. Klaassen, and Jeffrey I. Steinfeld

Citation: J. Chem. Phys. **96**, 8236 (1992); doi: 10.1063/1.462878
View online: http://dx.doi.org/10.1063/1.462878
View Table of Contents: http://jcp.aip.org/resource/1/JCPSA6/v96/i11
Published by the American Institute of Physics.

State-to-state rotational energy-transfer measurements in the $v_2 = 1$ state of ammonia by infrared–infrared double resonance

Bernd Abel,[a] Stephen L. Coy, Jody J. Klaassen, and Jeffrey I. Steinfeld
Department of Chemistry and G. R. Harrison Spectroscopy Laboratory, Massachusetts Institute of Technology, Cambridge, Massachusetts 02139

(Received 5 February 1992; accepted 28 February 1992)

An infrared double-resonance laser spectroscopic technique is used to study state-resolved rotational (R–R, R–T) energy transfer in ammonia ($^{14}NH_3$) (self-collisions and between ammonia and foreign gases). NH_3 molecules are prepared in selected rovibrational states of the $v_2 = 1$ level using coincidences between CO_2-laser lines and ν_2 fundamental transitions. Measurements of both the total rate of depopulation by collisions, and the rates of transfer into specific final rovibrational states (v,J,K) have been carried out using time-resolved tunable diode laser absorption spectroscopy. For NH_3–NH_3 collisions, measurements of total depopulation rates of selected JK states in $v_2 = 1$ and ground-state recovery rates are found to be three and eight times larger, respectively, than the Lennard-Jones collision rate, in accord with theoretical expectations for polar molecules. A kinetic master-equation analysis of time-resolved level populations yields state-to-state rate constants and propensity rules for NH_3–NH_3 and NH_3–Ar collisions. Individual rotational energy-transfer rates in $v_2 = 1$ are slower than in the vibrational ground state, but still comparable to the Lennard-Jones collision frequency. Our experiments show that rotational energy transfer in $v_2 = 1$ is not governed by simple "dipolelike" selection rules. They show fast rotational energy transfer, which can be related to long-range interaction potentials, but at the same time considerable amounts of $\Delta J = 2$ and 3, $\Delta K = 0$, and $\Delta J = 1$–4, $\Delta K = 3$, transitions, which may be attributed to higher-order terms in the multipole expansion of the intermolecular potential. No pronounced symmetry-state correlation and no preferred pathways were found except the preference for relaxation within a K stack and the expected separate relaxation of different nuclear-spin species, which can be labeled by their K-quantum number. Rates of collision-induced symmetry change ($a \leftrightarrow s$) in $v_2 = 1$ are on the order of $k_{as} = 4\ \mu s^{-1}\ torr^{-1}$, smaller than k_{as} in the ground state, but over an order of magnitude larger than that recently reported in the literature. Depopulation rates for other collision partners (Ar, H_2, N_2, and He) can be understood in terms of the intermolecular potentials. Comparisons are made between the relaxation rates measured in this work and infrared pressure-broadening coefficients reported in the literature.

I. INTRODUCTION

The ammonia molecule has been the subject of numerous investigations utilizing time-resolved spectroscopy to elucidate energy-transfer and relaxation processes occurring among the rotational and vibrational energy levels of this molecule.[1] In the vibrational ground state of ammonia, each rotational state is split by inversion doubling into a pair of levels of opposite (a and s) parity, between which dipole-allowed transitions occur in the 15–40 GHz region. This is a convenient region for microwave spectroscopy, which has been extensively utilized to study rotational relaxation in the vibrational ground state of ammonia by microwave double-resonance techniques.[2] As the ammonia molecule is excited in its ν_2 out-of-plane mode, the inversion splitting progressively increases. The vibrational fundamental $\nu_2 \leftarrow 0$ coincides with several CO_2 and N_2O laser lines, affording a convenient excitation method for transient nutation[3] and time-resolved infrared-microwave double-resonance[4–7] experiments on ammonia. The vibrational and rotational spectra of ammonia are also of interest for remote-sensing measurements, e.g., in terrestrial combustion systems[8] and the atmospheres of the outer planets.[9]

In addition to the microwave double-resonance experiments noted above,[2–7] a number of molecular-beam scattering measurements have been carried out on state-to-state rotational energy-transfer processes in the vibrational ground state of ammonia. Klaassen *et al.*[10] investigated rotational- and symmetry-state-changing collisions in a molecular-beam maser. Meyer, Buck, and co-workers[11] studied rotationally inelastic scattering with H_2 and He as collision partners, but these experiments were carried out at relatively high collision energies (0.075–0.01 eV, corresponding to 600–800 cm^{-1} or an effective temperature of 800–1200 K). Recently, Schliepen and ter Meulen[12] prepared the 0_0^+ state of ortho-NH_3 with a quadrupole field selector in a molecular beam. They used resonantly enhanced multiphoton ionization to obtain rotational excitation cross sections for collisions with He and H_2.

In contrast to the vibrational ground state, data on the

[a] Present address: Institut für physikalische Chemie, Tammannstrasse 6, Göttingen, Germany.

 0021-9606/92/118236-15$06.00

details of rotational energy transfer in the vibrational excited states of ammonia are much less extensive. The time-resolved infrared double-resonance (TRIRDR) technique, using a pulsed CO_2 laser to pump rovibrational transitions and a tunable infrared diode laser as a probe, has been employed in our laboratory[13–15] and elsewhere to obtain highly detailed descriptions of state-to-state energy transfer among rotational levels in excited vibrational states of small polyatomic molecules. Such experiments have not been carried out on ammonia. Reid and co-workers[16,17] used this technique to measure vibrational relaxation in the $v_2 = 1$ and 2 levels of ammonia, but at high gas pressures at which rotational relaxation was essentially complete on the time scale of the measurements. Schwendeman and co-workers[18(a)] carried out infrared double-resonance experiments on ammonia using a sideband-modulated CO_2 laser as a probe, which did not have the tuning range necessary to probe a large number of rotational levels. Their earlier microwave measurements evaluated T_2/T_1 in the ground state for a large number of levels.[18(b)–18(d)] Veeken, Dam, and Reuss[19] carried out infrared double-resonance experiments (using a color-center laser as a probe) on expansion-cooled ammonia, obtaining overall population relaxation times and symmetry-changing collision rates in the ground and excited vibrational levels.

Resonantly enhanced multiphoton ionization (REMPI) spectroscopy has also been used[20,21] to follow relaxation in vibrationally excited levels of ammonia following infrared pumping. Using this technique, Shultz and Wei[20] reported a rate coefficient for collision-induced transfer between a and s levels in the vibrationally excited state, $k_{as}(v_2 = 1) = 0.21 \times 10^6\ \mathrm{s}^{-1}\ \mathrm{torr}^{-1}$, about 50 times slower than the "hard-sphere" collision rate. This is a quite unexpected result, since symmetry-changing collisions should be a strongly dipole-allowed process, and indeed in the vibrational ground state, $k_{as}(v_2 = 0)$ has been found to contribute on the order of 50% to the line-broadening rates for low J levels[1–5,18(b)–(d),19] where the line-broadening rates range between 110 and 160 $\mu\mathrm{s}^{-1}\ \mathrm{torr}^{-1}$. Furthermore, in recent "triple-resonance" experiments on the $v_2 = 2$ level of ammonia,[22] we found a lower limit for $k_{as}(v_2 = 2)$ of 2 $\mu\mathrm{s}^{-1}\ \mathrm{torr}^{-1}$, and it is expected that k_{as} would be *smaller* in $v_2 = 2$ than in $v_2 = 1$, because of the larger inversion splitting in $v_2 = 2$.

On the basis of the first Born approximation in scattering theory, rotational energy transfer in ammonia might be expected to follow dipolelike propensity rules, i.e., $\Delta J = 0, \pm 1$ and $\Delta K = 0$, with change in parity. While this is a useful approximation for ammonia colliding with polar molecules, deviations from this behavior have been well documented in the earlier microwave double resonance work.[2,7,12,23]

Since no systematic study of rotationally inelastic processes in the vibrationally excited state of ammonia is available, and in order to resolve some of the discrepancies noted above, we undertook a series of time-resolved infrared double-resonance experiments on ammonia, in which we determined state-to-state rotational energy-transfer thermal rate coefficients and propensity rules in the excited $v_2 = 1$ state, including the symmetry-changing ($a \leftrightarrow s$) process. These results are presented here, along with comparisons of our results with other work reported in the literature. In particular, the measured inelastic collision rates are compared with self- and hydrogen-pressure-broadening coefficients for the ammonia $\nu_2 \leftarrow 0$ band,[24–27] which are of particular importance to remote-sensing measurements of the outer planets,[9] and with theoretical models.

II. EXPERIMENT

The IR–IR double-resonance setup has already been described in recent publications.[13,14,22] Only those modifications which have been made in the present experiment will be described here. Briefly, a pulsed line tunable CO_2 laser is used as the pump source, in conjunction with a tunable diode laser probe. The pump laser is a grating tuned TE CO_2 laser (Laser Science, Inc. PRF-150S) with a typical pulse energy of 50 mJ/pulse and a pulsewidth of 80–100 ns [full width at half maximum (FWHM)]. The estimated bandwidth is about 4 GHz. In order to avoid complications from long afterpulses the laser was operated at low N_2 partial pressure. Unless otherwise noted the CO_2 laser is set to the $10P(32)$ (932.960 cm^{-1}) or the $9R(30)$ (1084.635 cm^{-1}) line, which are coincident with the fundamental $aQ(5,3)$ and $sR(5,0\text{–}3)$ transitions in ammonia. The mismatches between the two laser lines and the $\nu_2 \leftarrow 0$ transitions are 0.95 and 0.2 GHz, respectively, ensuring efficient near-resonant pumping. For the transient absorption measurements of population prepared in $v_2 = 1$, we used a 10 μm PbSeTe diode laser (Laser Photonics Analytics Division) operated at 35–50 K at a current of 200–700 mA. The multimode output of the 10 μm diode was collimated with a 2 in. focal length lens ($f/1$) and passed through a polarizer oriented with its axis approximately orthogonal to the polarization axis of the pump beam in order to prevent scattered pump light perturbations to the diode. The pump-and-probe beam polarizations were thus approximately perpendicular throughout the double-resonance volume. The bandwidth of the diode had previously been determined to be approximately 0.0004 cm^{-1} by least-squares fitting of self-broadened infrared absorption lines of ozone.[28]

The approximately collinear (within 1°–2°) counterpropagating cw diode laser beam and the CO_2 laser pulse were overlapped in a static stainless-steel cell. The two beams were separated behind the cell using a grating. After the separation the diode laser beam passed through a 0.5 m monochromator (Bausch & Lomb) which isolated the mode of interest in the wavelength region between 950 and 1080 cm^{-1}. The diode laser beam was then focused onto a HgCdTe detector [Santa Barbara Research (SBR), $\approx$50 ns rise time]. A confocal Fabry–Pérot étalon (Tec-Optics, FSR: 0.010 05 cm^{-1}) was inserted into the beam path behind the monochromator to provide a frequency reference, calibrated against standard lines taken from Ref. 29. The detector output was amplified with a SBR amplifier, monitored, and averaged on a digital averaging oscilloscope (Le Croy 9400A). Typically 500–1000 traces were averaged for an acceptable signal-to-noise ratio. The data were transferred to a microcomputer for further processing.

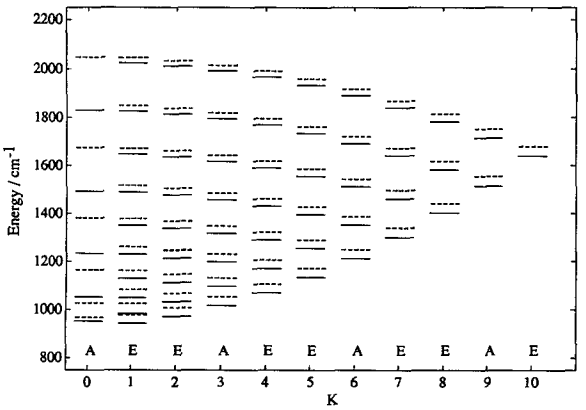

FIG. 1. Rotational level structure of ammonia in the $v_2 = 1$ level; a and s inversion levels are marked by dashed and solid lines, respectively.

The sample cell is a stainless-steel tube 2 m in length, with an inside diameter of 3.5 cm, equipped with antireflection coated ZnSe windows. NH_3 (Matheson) pressures in the cell between 3 and 50 mtorr were measured with a capacitance manometer (MKS Baratron, model 227A, 0–1 torr range). Gases used in the energy-transfer measurements were research-grade materials obtained from Matheson or Air Products.

III. SPECTROSCOPIC CONSIDERATIONS

In order to obtain a detailed picture of rotational energy transfer (R–R, R–T) in $v_2 = 1$, it is necessary to prepare and probe as many rovibrational levels as possible (see Fig. 1). Using a line tunable CO_2 laser we are limited in the number of levels that can be prepared. This limitation can partially be overcome by using ammonia coincidences with other gas laser transitions, e.g., N_2O (Refs. 3–7) or isotopic CO_2,[30] Stark-tuning the ammonia transitions into resonance,[31] or using isotopically substituted ammonia (e.g., $^{15}NH_3$).[32] Nevertheless, using just the well-known coincidences between the $9R(30)$ and $10P(32)$ lines of the $^{12}CO_2$ laser and the $aQ(5,3)$ and $sR(5,0\text{-}3)$ $\nu_2 \leftarrow 0$ transitions in $^{14}NH_3$, we have been able to prepare JK states having (a) different nuclear-spin species, (b) different parity (a,s) states, and (c) different rotational (J,K) states in $v_2 = 1$. These transitions also play an important role in infrared multiple-photon excitation of ammonia[22,33–36] and in the optically pumped ammonia laser.[37–40]

Fortunately, the spectroscopy of the symmetric bend vibration of NH_3 has been extensively studied in the past. Rovibrational assignments and frequencies for $v_2 = 1$, 2, and 3 are available from studies of Urban *et al.*[41–43] The transition frequencies of the $\nu_2 \leftarrow 0$ and $2\nu_2 \leftarrow \nu_2$ bands have been calculated using their assignments and assuming selection rules for parallel band transitions.

The 10 μm diode used in this work has a frequency range between 940 and 1088 cm^{-1}, which enabled us to probe the $s(J,0)$ and $s(J,3)$ rovibrational states shown in Fig. 1 up to $J = 7$. A summary of all pumped and probed levels, transitions, and frequencies is given in Table I.

IV. RESULTS

The $10P(32)$ line of the CO_2 laser at 932.960 cm^{-1} is coincident with the $\nu_2 \leftarrow 0$ $aQ(5,3)$ transition in ammonia.

TABLE I. Pump and probe transitions in NH_3 $\nu_2 \leftarrow 0$ band. For pump transitions, the offsets from line center are also given.

CO_2 pump	Frequency (cm^{-1})	NH_3 transitions	$\delta\nu$ (cm^{-1})
$10P(32)$	932.960	$s(5,3) \leftarrow a(5,3)$ [$aQ(5,3)$]	0.032
$9R(30)$	1084.635	$a(6,0) \leftarrow s(5,0)$ [$sR(5,0)$]	0.007
		$a(6,1) \leftarrow s(5,1)$ [$sR(5,1)$]	0.010
		$a(6,2) \leftarrow s(5,2)$ [$sR(5,2)$]	0.025

Probed levels	Probe transitions	ν (cm^{-1})
Ground state ($\nu_2 \leftarrow 0$ transitions)		
$a(5,3)$	$s(6,3) \leftarrow a(5,3)$ [$aR(5,3)$]	1053.1304
$s(5,1)$	$a(5,1) \leftarrow s(5,1)$ [$sQ(5,1)$]	966.5324
$v_2 = 1$ ($2\nu_2 \leftarrow \nu_2$ transitions)		
$s(5,3)$	$2a(6,3) \leftarrow s(5,3)$ [$2sR(5,3)$]	1058.8584
$s(6,1)$	$2a(7,1) \leftarrow s(6,1)$ [$2sR(6,1)$]	1070.9098
$s(7,3)$	$2a(8,3) \leftarrow s(7,3)$ [$2sR(7,3)$]	1088.7434
$s(6,3)$	$2a(7,3) \leftarrow s(6,3)$ [$2sR(6,3)$]	1074.0258
$s(4,3)$	$2a(5,3) \leftarrow s(4,3)$ [$2sR(4,3)$]	1043.1512
$s(3,3)$	$2a(4,3) \leftarrow s(3,3)$ [$2sR(3,3)$]	1026.8147
$s(5,0)$	$2a(6,0) \leftarrow s(5,0)$ [$2sR(5,0)$]	1055.0956
$s(3,0)$	$2a(4,0) \leftarrow s(3,0)$ [$2sR(3,0)$]	1022.7527
$s(1,0)$	$2a(2,0) \leftarrow s(1,0)$ [$2sR(1,0)$]	987.7378

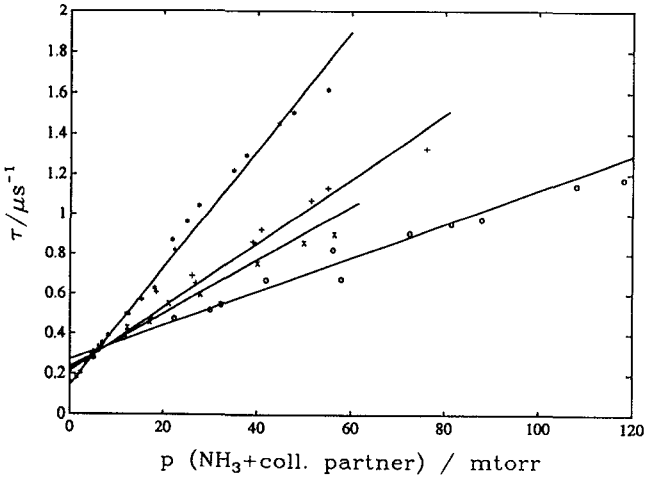

FIG. 2. Plot of $v_2 = 1$ $s(5,3)$ depopulation rates vs pressure for ammonia self- and foreign-gas relaxation. Points are denoted as follows: *, NH_3–NH_3; +, NH_3–N_2; ×, NH_3–H_2; O, NH_3–Ar.

Using this excitation wavelength only the $s(5,3)$ level in $v_2 = 1$ is populated (see Table I); this pump frequency has been used for most of the experiments described here. The $9R(30)$ line at 1084.635 cm^{-1} is coincident with the $sR(J = 5; K = 0, 1, 2,$ and $3)$ transitions in ammonia resulting in a much less selective population of $v_2 = 1$. Nevertheless, the $9R(30)$ line enabled us to carry out a direct measurement of the transition rate between a and s levels of $J = 6$ and $K = 1$ in $v_2 = 1$.

With use of the $10P(32)$ pump transition, the prepared s levels could be probed directly with the diode laser. In addition to these three-level double-resonance (DR) signals, we observed a large number of four-level DR signals, which are also listed in Table I. Measured inverse relaxation times k_Γ (μs^{-1} $torr^{-1}$) were converted to rate coefficients k_σ (cm^3 s^{-1}) and effective cross sections using the ideal-gas law and the standard relationship

$$\sigma_{\rm rot} = k_\sigma/(8kT/\pi\mu)^{1/2}, \quad (1)$$

where μ is the collision reduced mass. Numerically, k_Γ (μs^{-1} $torr^{-1}$) is equal to 0.282σ (Å^2) for NH_3–NH_3 at 293 K.

A. Total depopulation and ground-state recovery rates

Rates for removal of population from the $s(5,3)$ level in $v_2 = 1$, summed over all final states, after CO_2 laser excitation were determined by monitoring the absorption on the $2sR(5,3)$ $(2\nu_2 \leftarrow \nu_2)$ transition for a series of pressures. A plot of the signal relaxation time τ vs p gave a total depopulation rate for the $s(5,3)$ level of 34 ± 4 μs^{-1} $torr^{-1}$. A ground-state recovery rate of 80 ± 25 μs^{-1} $torr^{-1}$ for the $a(5,3)$ level was determined by the same procedure, monitoring the $aR(5,3)$ transition of $\nu_2 \leftarrow 0$. Total depopulation and ground-state recovery rates for both the upper and lower states of the fundamental transition $aQ(5,3)$ in ammonia were determined. They enable us to compare the average relaxation rates of the upper and lower levels with pressure-broadening coefficients of this transition, as will be done in the discussion. With use of the different collision partners, depopulation rates of the $s(5,3)$ in $v_2 = 1$ were determined by a fit of a sum of two exponentials to the data. Although the contribution of feedback from adjacent levels makes this result somewhat ambiguous, the longer time constant includes diffusion and free-flight losses of the excited molecules, while the shorter time constant more closely approximates the phenomenological depopulation rate which we wish to extract from the data. A more detailed discussion of this point occurs below. The depopulation results are shown in Fig. 2. Table II gives a summary of measured ground-state recovery and total $v_2 = 1$ depopulation rates for NH_3–NH_3 collisions, and total $v_2 = 1$ depopulation rates in the presence of foreign gas collision partners. These depopulation measurements, like all the transients measured in this study, were performed with pump-and-probe polarizations perpendicular.

B. Symmetry changing collisions

For direct measurements of a–s transfer the $[v_2 = 1, a(6,1)]$ state has been excited and probed via the $sR(6,1)$ $2\nu_2 \leftarrow \nu_2$ transition. Figure 3 shows a transient absorption signal measured for the $s(6,1)$ level, along with the prediction for the time variation of the population in this level from the kinetic model described in the following section. Although this measurement is not free from interferences of other levels due to the population of the levels $a(6,0)$,

TABLE II. Total depopulation rates for $s(5,3)$, $v_2 = 1$ and ground-state recovery rates for $a(5,3)$.

	k_Γ (μs^{-1} $torr^{-1}$)	k_σ (cm^3 s^{-1})	σ (Å^2)
Ground-state recovery [$a(5,3)$]			
NH_3–NH_3	80 (20)	$25\ (6) \times 10^{-10}$	291 (75)
Total depopulation [$v_2 = 1$, $s(5,3)$]			
NH_3–NH_3	34 (4)	$10.7\ (1.3) \times 10^{-10}$	123 (14)
NH_3–N_2	16 (2)	5.0 (0.6)	65 (8)
NH_3–H_2	13.4 (2)	4.2 (0.6)	22 (3)
NH_3–Ar	8.5 (2)	2.7 (0.6)	36 (8)
NH_3–He	6 (3)	1.9 (0.9)	13.5 (7)

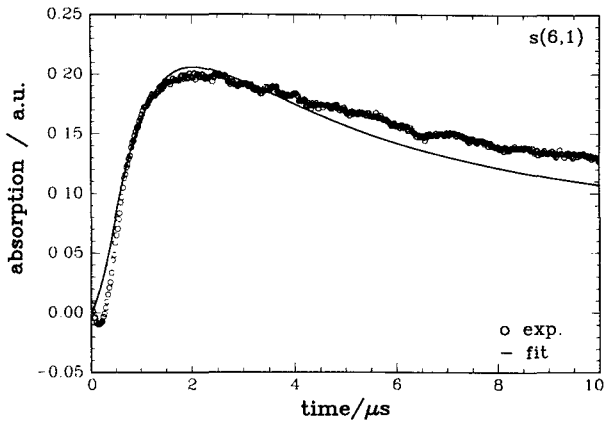

FIG. 3. Four-level DR signal showing rapid $a \rightarrow s$ parity-changing collisions in ammonia (15.2 mtorr). The $9R(30)$ CO_2 laser line pumps the $a(6,1)$ level in $v_2 = 1$, and the probed transition is $sR(6,1)$, $2v_2 \leftarrow v_2$. The solid curve is the prediction of the kinetic model described in the text. This should be compared with Fig. 8 of Ref. 20.

$a(6,1)$, and $a(6,2)$, it provides a direct measurement of the $a \rightarrow s$ transfer rate, which is estimated from the model to be 4 μs^{-1} torr^{-1}.

C. State-to-state rotational energy transfer

In this section we examine rotational (R–R, R–T) energy transfer in $v_2 = 1$. In this region V–V and V–T,R energy transfer is slow and can be neglected.[16] The initially excited levels are $v_2 = 1$, $s(5,3)$ and $a(6,0)$. Measurements were made at NH_3 pressures between 5 and 50 mtorr. A complete list of observed transitions has been given in Table I.

1. Nuclear-spin restrictions on collisional energy transfer

Each rotational level in $^{14}NH_3$ is associated with a characteristic nuclear-spin wave function. The different nuclear-spin species are labeled as A and E for the ortho and para species and can be distinguished by their K quantum number (K is an integer multiple of 3 for the A species, the other K values are of E symmetry). Since the nuclear spins are not effectively relaxed by collisions, the symmetry species cannot interconvert under our experimental conditions except via exchange collisions. The rigorous collision propensity rule $A \leftrightarrow A$ and $E \leftrightarrow E$, all others forbidden, was checked by preparing the $s(5,3)$ and probing the $s(5,2)$ level of NH_3. From the small amplitude of the observed signal, we estimated an upper bound of $k(A \leftrightarrow E) < 0.5$ μs^{-1} torr^{-1} for collisional transfer between these levels with different nuclear-spin wave functions. Resonant exchange between A and E species has been reported for other systems,[44,45] and resonant vibrational exchange transfering excitation between NH_3 spin species has been measured by Danagher and Reid[16] to be 0.69 μs^{-1} torr^{-1}. Their result is a total rate obtained without rotational resolution, so our state-to-state rate is, as expected, somewhat lower, and is sufficiently low to neglect in the model.

2. Simple kinetic model for absorption time profiles using a master-equation approach

In order to obtain quantitative estimates of the state-to-state energy-transfer rates, we used a master-equation approach[46–48] which enables us to model population transfer among a specified set of levels. If $\mathbf{N}$ is the array of level populations and $\mathbf{K}$ is the matrix of rates connecting these levels, the time evolution of $\mathbf{N}$ is given by

$$\dot{\mathbf{N}} = \mathbf{K}\mathbf{N}. \tag{2}$$

Although the initial and final states are completely resolved in our experiments, the complete state-to-state rate matrix $\mathbf{K}$ can be obtained only by modeling the population changes in the detected levels. This is an inherent problem of this type of experiment, in which one is always summing over a number of possible pathways connecting the initial and final states.[13,14,49] The array of time-varying populations $\mathbf{N}(t)$ in Eq. (2) can be obtained either by calculating the eigenvalues of $\mathbf{K}$ or by integrating the set of coupled differential equations. In the latter case, the set of equations (2) which has to be integrated can be written as

$$dN_i/dt = \sum_{j \neq i} k_{ij} N_j + k_{ii} N_i = \sum_j k_{ij} N_j, \tag{3}$$

where k_{ij} is the rate of transfer of population from level j to level i, and the depopulation rate of level i, k_{ii}, is related to the rates of transfer of population into the level by the conservation criterion:

$$k_{ii} = -\sum_{j \neq i} k_{ij}. \tag{4}$$

Total depopulation rates of the directly pumped level (see Sec. IV A) are in this sense eigenvalues of the rate matrix $\mathbf{K}$.[46,47] In the equation for the directly pumped level, a term has been added to account for the time-dependent population of this level by the CO_2 laser:

$$dN_p/dt = \sum_{\text{all } j} k_{pj} N_j + \alpha I(t), \tag{5}$$

where $I(t)$ is the experimental pulse profile and α is a phenomenological proportionality coefficient.

In order to reduce the number of energy levels and differential equations which need to be considered, we used a simplified model for rotational energy transfer in $v_2 = 1$ of NH_3. First, we expect the interconversion of nuclear-spin species to be slow on the time scale of our experiments. Indeed, Oka[2] argues that the transition between *ortho* and *para* species of ammonia should be strictly forbidden. Since we have verified this experimentally (see the preceding section), we assumed that the interconversion propensity rule holds strictly, and included in the model only states of the same nuclear-spin species as the initially pumped level. States with $J > 8$ ($K = 0$, 3, and 6), and all states with $K = 9$, were grouped together into four baths of states which were not allowed to feed back into the system of levels in the numerical model. These simplifications and assumptions resulted in a condensed system with 30 equations in which every pair of J,K states with $J < 9$ and $K < J$ could be explicitly taken into account. Eight of the s levels in the case of $aQ(5,3)$ excitation, three s levels in the case of $sR(5,0)$ exci-

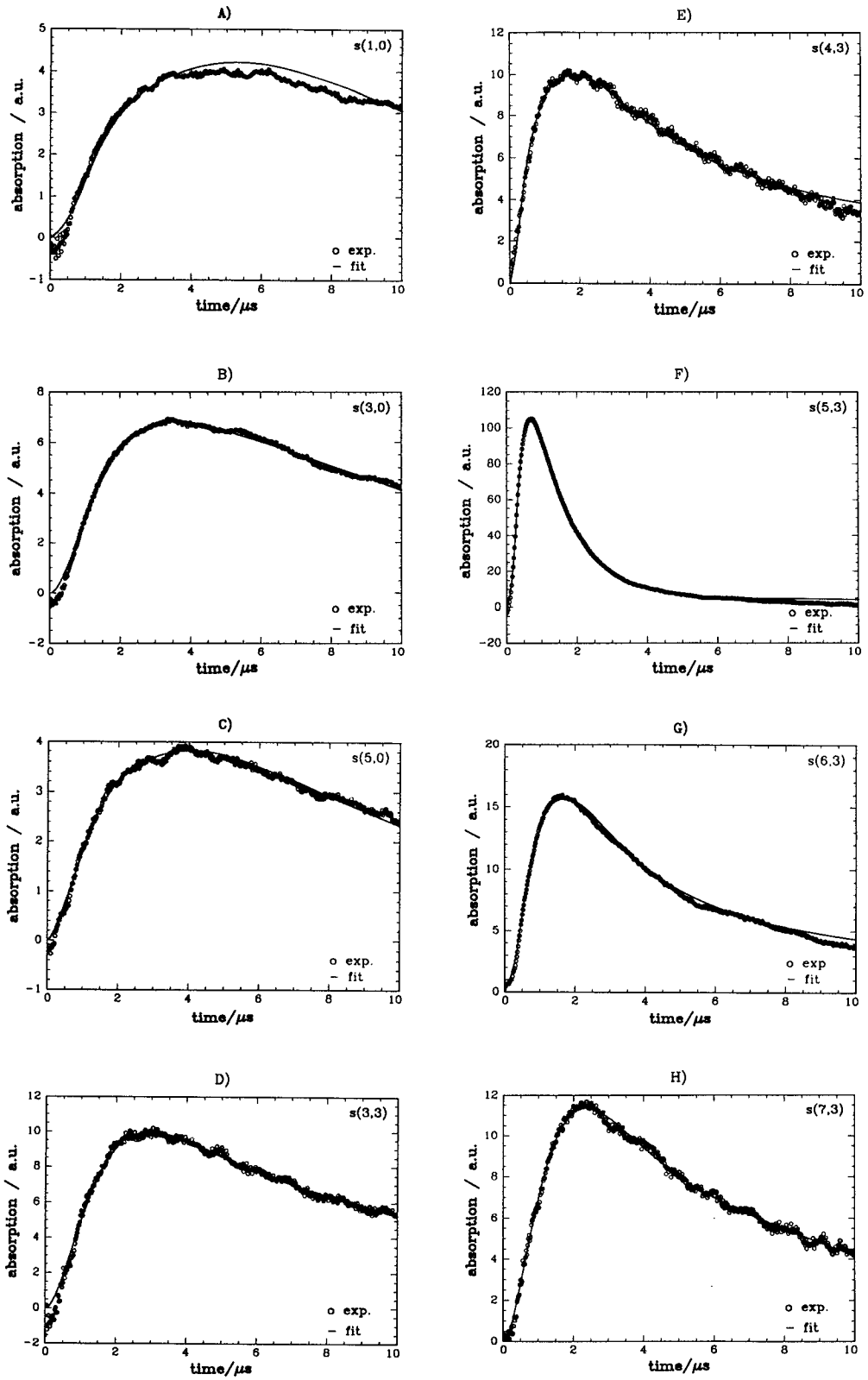

FIG. 4. Three- and four-level DR signals in ammonia (25 mtorr). The $10R(32)$ CO_2 laser line pumps the $s(5,3)$ level in $v_2 = 1$. The levels probed are (a) $s(1,0)$, (b) $s(3,0)$, (c) $s(5,0)$, (d) $s(3,3)$, (e) $s(4,3)$, (f) $s(5,3)$ (showing total relaxation out of pumped level), (g) $s(6,3)$, and (h) $s(7,3)$. The symbols (O) are experimental points; the solid curve is the fit to the master-equation model described in the text. Note in panel (f) the slow decrease in absorbance (population) at long times ($>7\,\mu s$), due to the loss of vibrationally excited molecules resulting from transport out of the beam and V–T relaxation which is not explicitly included in the kinetic model.

tation, and one a–s transition ($J=6$, $K=3$) could be probed directly, resulting in a large number of observables compared to the parameters to be determined.

Using this model, we determined rate coefficients $k(a\leftrightarrow s)$, $k(\Delta J,\Delta K=0)$ and $k(\Delta J,\Delta K=-3)$ for NH_3–NH_3 and NH_3–Ar collisions. Even though levels resulting from $\Delta K=+3$ changes were not directly monitored, parameter values could be estimated for these channels in the context of the global model; they make a small but non-negligible contribution to the total relaxation process. The downward rates for the $(\Delta J,\Delta K=0)$ processes were represented by a simple exponential-gap scaling law, but those for $(\Delta J,\Delta K=3)$ processes could not be satisfactorily scaled using either an exponential-gap or power-gap law,[50–52] and were therefore fitted individually. The average rate coefficient for the $a\leftrightarrow s$ symmetry changing process was fitted independently. Upward rate coefficients were calculated by detailed balancing. The cutoff for ΔJ in our model was $|\Delta J_{\max}|=4$, and that for ΔK was $|\Delta K|=3$; these seemed to be reasonable choices for a polar molecule which might be supposed to follow "dipolelike" propensity rules. We first tried to incorporate the $a\leftrightarrow s$ propensity rule into the model, but we were unable to reproduce the data satisfactorily under this constraint. Ultimately, we allowed both symmetry-changing and symmetry-preserving collisions to take place, with a variable ratio $\beta=k(a\leftrightarrow a)/k(a\leftrightarrow s)=k(s\leftrightarrow s)/k(a\leftrightarrow s)$.

The master equation was integrated numerically with a FORTRAN program using a standard Runge–Kutta algorithm with adaptive step size.[53] The system response was taken into account by convoluting the calculated signal with an experimentally determined response function. Minor losses due to vibrational relaxation and transport out of the detection region have not been included in the model; their effect may be noted in Fig. 4(f).

The parameter values which gave the best overall correspondence with the measured curves for NH_3–NH_3 collisions, as shown in Figs. 4(a)–(h), are given in Table III, and those for NH_3–Ar collisions [Figs. 5(a)–(c)], are given in Table IV. In Tables III and IV we also show the sums of the inelastic rate coefficients for two values of the ratio β defined above, viz., $\beta=1.0$ (symmetry-changing and symmetry-preserving collisions equally likely) and $\beta=0.7$. While it was not possible to determine a precise value for β, it is nevertheless clear from the fits that a substantial fraction of the rotationally inelastic collisions in $v_2=1$ must preserve the (a,s) symmetry, in contradiction to a simple dipole-propensity model. The sums may be compared with the total relaxation rates reported in Table II, $34\pm4\,\mu s^{-1}\,torr^{-1}$ for NH_3–NH_3 collisions, and $8.5\pm2\ \mu s^{-1}\,torr^{-1}$ for NH_3–Ar. Since these relaxation rates, which are eigenvalues of the rate coefficient matrix $\mathbf{K}$, are always expected to be slightly smaller than the sum Σk_{ij} [Eq. (4)], as a result of "feedback" from populated nearby levels, they furnish a definite, albeit not very precise, lower bound on β of about 0.7 for NH_3–NH_3 and about 0.6 for NH_3–Ar.

Once a suitable set of energy-transfer parameters for the $aQ(5,3)$ excitation had been determined, the set of rate coefficients was used to model the experimental traces for $sR(5,0)$ excitation. The calculated curves match the experi-

TABLE III. Energy-transfer parameters for NH_3–NH_3 rotational energy transfer within $v_2=1$ with the initial level: $v_2=1$, $s(5,3)$, at 298 K. The rates given are those for parity-changing collisions (change of inversion level). The parity-conserving transitions are related by the parameter β, which gives the ratio of parity-conserving to parity-changing transitions, and is estimated to be between 0.7 and 1.0.

$\Delta J,\Delta K$	k_Γ ($\mu s^{-1}\,torr^{-1}$)	k_σ ($cm^3\,s^{-1}$)
Directly observed, rates for parity-changing transitions		
+3,0	0.25	0.08×10^{-10}
+2,0	0.67	0.21
+1,0	3.87	1.22
0,0	4	1.26
−1,0	5.71	1.79
−2,0	2.21	0.69
+3,−3	0.12	0.038×10^{-10}
+2,−3	0.29	0.09
+1,−3	0.69	0.22
0,−3	1.5	0.47
−1,−3	1.1	0.35
−2,−3	0.90	0.28
−3,−3	0.78	0.24
−4,−3	0.70	0.22
Predicted by model, rates for parity-changing transitions		
+1,+3	0.80	0.26×10^{-10}
+2,+3	0.35	0.11
+3,+3	0.15	0.05
$\Sigma k_{ij}=38.1\,\mu s^{-1}\,torr^{-1}$ ($\beta=1$)		12.2×10^{-10}
$33.9\,\mu s^{-1}\,torr^{-1}$ ($\beta=0.7$)		

mental traces reasonably well without further adjustment [Figs. 6(a)–(c)], thus providing additional validation of the results obtained from the modeling.

From systematic variation of the rate coefficients, we have estimated an overall error limit of ± 20% for the resulting coefficients, which includes uncertainties due to the simplified model, the cutoff for ΔJ and ΔK, and losses due to vibrational energy transfer and diffusion. The key finding is that in order to reproduce the experimental data, nondipolar energy-transfer processes must be included in the model.

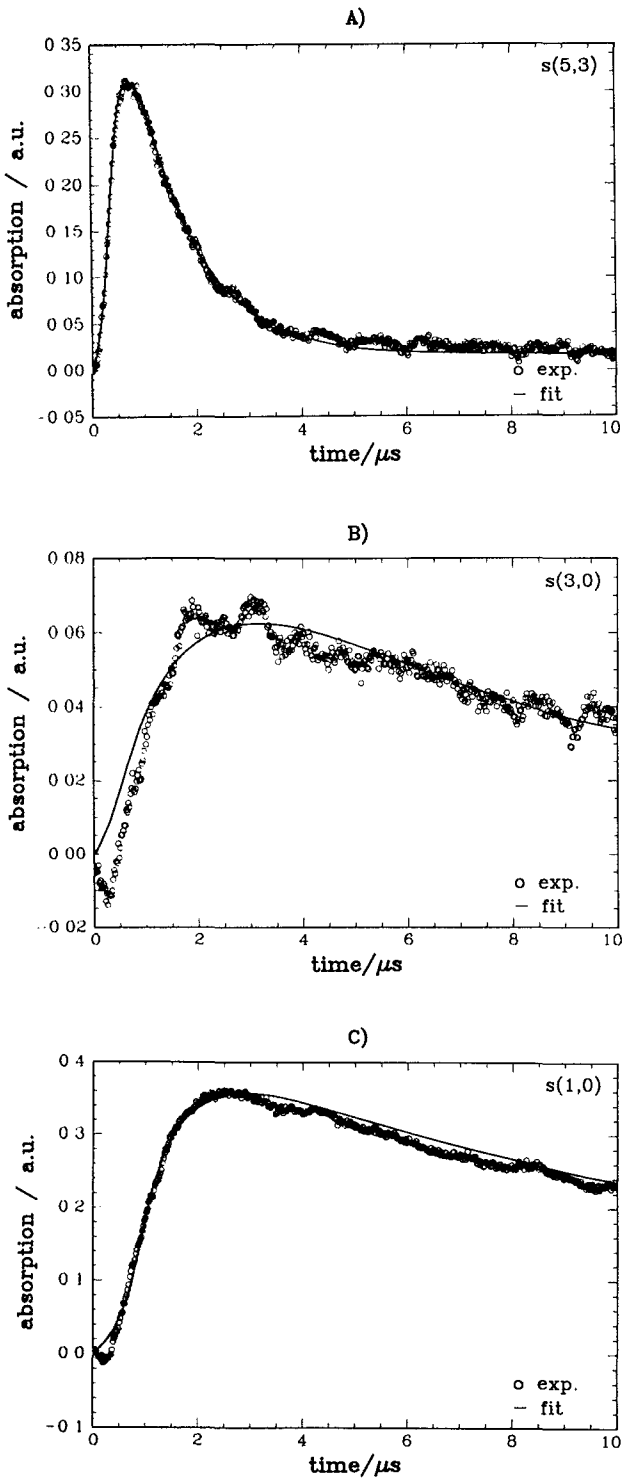

FIG. 5. Three- and four-level DR signals in ammonia–argon mixtures. The $10R(32)$ CO_2 laser line pumps the $s(5,3)$ level in $v_2 = 1$. The levels probed are (a) $s(5,3)$, 5 mtorr NH_3 + 56 mtorr Ar, showing total relaxation out of pumped level; (b) $s(3,0)$, 25 mtorr NH_3 + 100 mtorr Ar; (c) $s(1,0)$, 16 mtorr NH_3 + 307 mtorr Ar. The symbols (O) are experimental points; the solid curve is the fit to the master-equation model described in the text.

TABLE IV. Energy-transfer parameters for NH_3–Ar rotational energy transfer within $v_2 = 1$ with the initial level: $v_2 = 1$, $s(5,3)$, at 298 K. The rates given are those for parity-changing collisions (change of inversion level). The parity-conserving transitions are related by the parameter β, which gives the ratio of parity-conserving to parity-changing transitions, and is estimated to be between 0.7 and 1.0.

$\Delta J,\Delta K$	k_Γ (μs^{-1} torr^{-1})	k_σ (cm^3 s^{-1})
directly observed, rates for parity-changing transitions		
+3,0	0.15	0.47×10^{-11}
+2,0	0.29	0.91
+1,0	1.07	3.37
0,0	1.18	3.72
−1,0	1.5	4.73
−2,0	0.75	2.36
+3,−3	0.04	0.13×10^{-11}
+2,−3	0.08	0.24
+1,−3	0.18	0.57
0,−3	0.37	1.16
−1,−3	0.29	0.91
−2,−3	0.24	0.75
−3,−3	0.21	0.65
−4,−3	0.19	0.59
predicted by model, rates for parity-changing transitions		
+1,+3	0.25	0.79
+2,+3	0.12	0.38
+3,+3	0.06	0.18
$\Sigma k_{ij} = 11.1\ \mu s^{-1}$ torr^{-1} ($\beta = 1.0$)		35.1×10^{-11}
$9.8\ \mu s^{-1}$ torr^{-1} ($\beta = 0.7$)		

V. DISCUSSION AND CONCLUSIONS

In this work, time-resolved infrared double resonance has been used to obtain a large set of state-to-state rate coefficients for rotational energy transfer in excited NH_3 vibrational states. The state-resolved collisional relaxation of ammonia rotational states in $v_2 = 1$ presents some interesting features, several of which will be considered in this section. The connection of "propensity rules" for J, K, M, and parity-changing collisions with the corresponding intermolecular interaction potentials, and with collision broadening of the $v_2 = 1 \leftarrow 0$ infrared transitions, will also be discussed.

A. Total depopulation rates and ground-state recovery rates

The total rotational relaxation and the ground-state recovery rates in NH_3 self-collisions are on the order of three to eight times the corresponding Lennard-Jones collision rates. This is comparable with results for CDF_3,[54] another symmetric-top molecule, but much more efficient than rotational relaxation in nonpolar molecules such as CHD_3 (Ref. 55) or spherical tops such as SF_6 (Ref. 56) and $^{13}CD_4$ (Ref. 13). The mechanism of the interaction between an ammonia

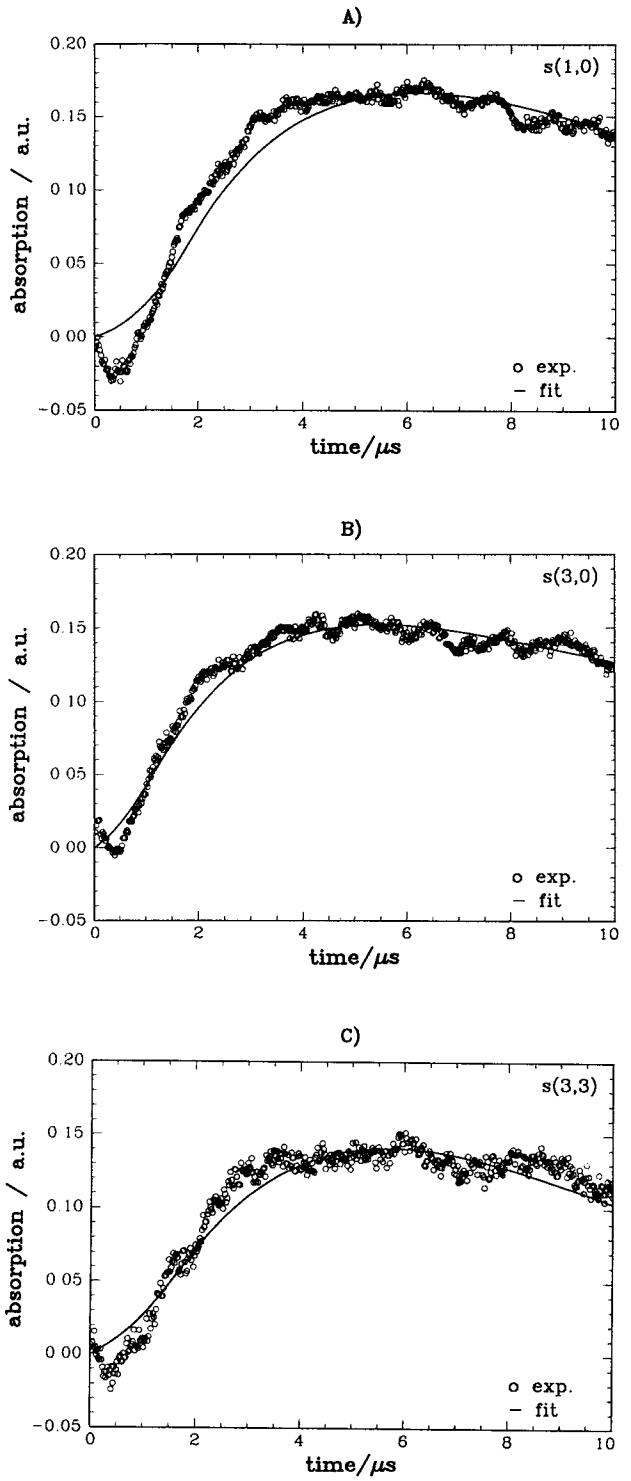

FIG. 6. Four-level DR signals in ammonia. The $9R(30)$ CO_2 laser line pumps (mostly) the $a(6,0)$ level in $v_2 = 1$. The levels probed are (a) $s(1,0)$, 23 mtorr; (b) $s(3,0)$, 33.6 mTorr; and (c) $s(3,3)$, 23 mtorr. The symbols (O) are experimental points; the solid curve is the fit to the master-equation model described in the text using the kinetic parameters derived from fitting the $s(5,3)$ data.

molecule and a rare-gas atom is expected to be quite different from that between two polar NH_3 molecules. First, in the NH_3–rare-gas collisions, the intermolecular interaction is caused by an induced moment or a fluctuation moment (which leads to a dispersion force) in a rare-gas atom while in the NH_3–NH_3 collision the main intermolecular interaction is caused by the long-range dipole–dipole force. Second is the effect of rotational resonances between incoming and outgoing channels in collision processes. Although rotational resonances are reduced in $v_2 = 1$ NH_3 colliding with ground-state NH_3 from the pervasive inversion-doublet resonance in ground-state–ground-state collisions, ΔJ resonances, and rotational inelasiticity in the perturber are still available to absorb energy, while in the NH_3–rare-gas case the energy defect must be supplied or dissipated by the translational motion of the rare-gas atom. The cross sections (averaged over thermal velocity distribution) for total depopulation in NH_3–Ar and NH_3–He collisions reflect this behavior. However, as will be discussed below, the state-to-state propensity rules differ from those which would be predicted by a simple first-order dipolar interaction.

B. Choice of rotational energy transfer model and rate-constant scaling

When using a kinetic model to determine rate coefficient parameters in a highly coupled system, it is especially important to consider the possible model dependence of the results.[49,57] The initial picture of rotational energy transfer in NH_3 was a very simple one. In addition to the rigorous propensity rules based on spin statistics, which allow the *ortho* ($K = 3n$) and *para* ($K \neq 3n$) levels to be treated separately, inelastic processes in NH_3 were expected to follow dipolelike behavior, viz., $\Delta J = 0,1$ and $\Delta K = 0$ with $a \leftrightarrow s$ being the only allowed channels.

Although these "dipolelike" propensity rules for collision-induced transitions are by no means as rigorous as optical selection rules, we expected to be able to model the experimental rotational energy-transfer data with a combination of fast $\Delta J = 0$ and 1, very slow $\Delta K = 3$, and very fast $a \leftrightarrow s$ transitions. However, we could not describe the rotational energy transfer in NH_3 with this model at all. A drastic relaxation of the constraints on the propensity rules resulted in a model which included $a \leftrightarrow a$ and $s \leftrightarrow s$, $\Delta K > 1$, and $\Delta J > 1$ transitions, with probabilities comparable to those of the "dipolelike" transitions. In principle, any level could be accessed by any other level within the nuclear-spin constraint.

An examination of the details of some of the kinetic fits will illustrate the validation of the model described above. If we look at the signal for $s(1,0)$ [Fig. 4(a)], we see an immediate increase in population after the CO_2 laser pulse; after 2 μs, the population of the $s(1,0)$ state has already reached half of its maximum value. If we do not assume ridiculously large cross sections for direct transitions from $s(5,3)$ to $s(1,0)$ (many times larger than the Lennard-Jones cross section), we have to allow for a considerable amount of $\Delta K = 3n$, $\Delta K, \Delta J$ transitions and perhaps s–s and a–a transitions. The s–s and a–a transitions are even more evident from the $s(4,3)$ and the $s(3,3)$ levels [Figs. 4(d) and 4(e)]. The rapid population of these levels cannot be explained by sequential $a \leftrightarrow s$ and $\Delta J = 1$ transitions. If we allow explicitly for $a \leftrightarrow a$ and $s \leftrightarrow s$ transitions the rate for the $s(5,3) \rightarrow s(4,3)$ or $s(6,3)$ and for $s(5,3) \rightarrow s(5,0)$ are the $\Delta J = 1$ and the

$\Delta K = 3$ transitions, respectively, in a first approximation. The measurement for $a(6,1) \rightarrow s(6,1)$ has been taken as a direct measure for the $a \leftrightarrow s$ transfer.

If we compare the traces for the population of the $s(5,3)$ and $s(4,3)$ or $s(6,3)$ levels, we can see the relative difference in the rates for $\Delta J = 1$ and $\Delta K = 3$ processes. The differences in the features of the population of $s(6,1)$ and the $a(6,1)$ ($a \rightarrow s$ transfer) are small. This means that the rate for $a \rightarrow s$ transfer is of the same order of magnitude than that for $\Delta J = 1$ transfer.

A further verification of the model is obtained by using the unadjusted parameters obtained from simulating the $aQ(5,3)$ excitation to predict the results of $aR(5,0)$ excitation. As Fig. 6 shows, quite satisfactory agreement is obtained.

A fundamental problem in rotational energy-transfer studies on polyatomic molecules is that the number N of levels, and especially the number $N(N-1)/2$ of collisional rates that connect these levels, can be large. Not only would it be difficult to measure all of these rates, it is especially unrealistic to vary every constant individually in simulating these systems. A more practical approach is to calculate the whole rate coefficient matrix by an angular-momentum-based scaling law with a set of basis rate constants. These can be obtained from coupled states, infinite-order sudden, or energy-corrected sudden approximation.[58] However, to date, the intermolecular potential for the NH_3 system has not been characterized well enough to be able to implement such an approach. Therefore it would be difficult to obtain *ab initio* basis rate constants for this system.

Scaling laws can therefore seldom be used to fit data for polyatomic molecules because there are so many basis rate constants that the number of free parameters in the fit becomes too large. Fitting laws represent the rate constants by simple functions which have a small number of adjustable parameters. For scaling the J-changing rate coefficients in our model, we used a simple and widely used exponential-gap law[50-52] (EGL) for downward transitions,

$$k_{j_i,-j_f} = (2j_f + 1)k_0 \exp[-C(E_i - E_j)/k_B T]. \quad (6)$$

The EGL has been given theoretical respectability by surprisal theory[59] and quantum-mechanical considerations, although this of course does not constitute a proof of the law. The EGL was found to work reasonably well for scaling the J-changing rates in NH_3–NH_3 and NH_3–Ar collisions.

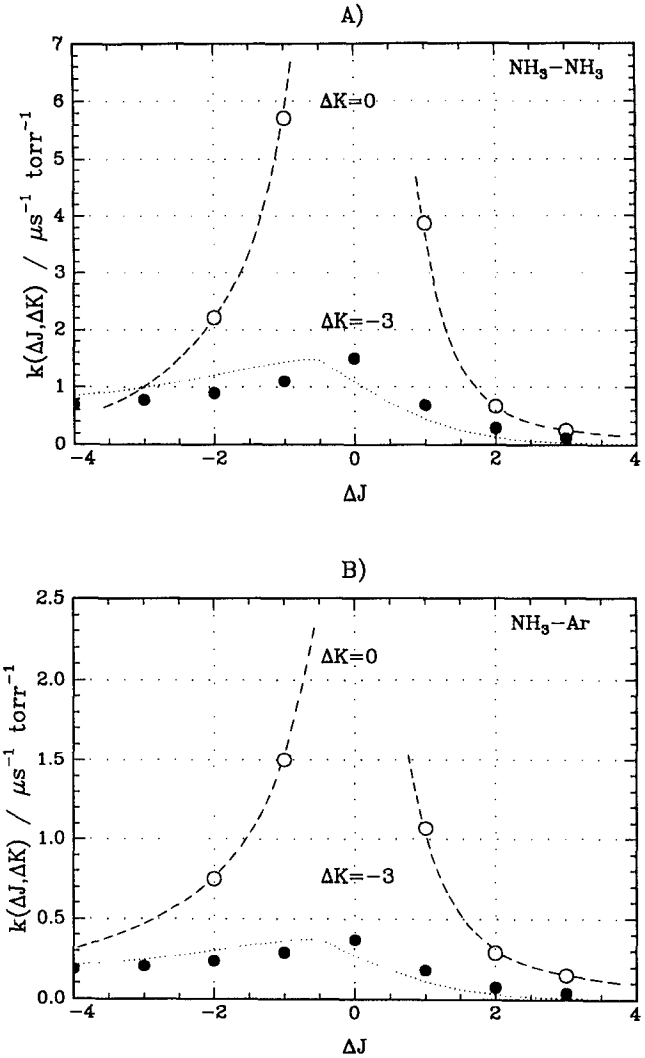

FIG. 7. Rate coefficients for J-changing collisions in (a) NH_3–NH_3 collisions and (b) NH_3–Ar collisions, as a function of ΔJ, with $\Delta K = 0$ (open circles) and 3 (solid circles). The dashed curve shows the EGL fit to the $\Delta K = 0$ rates, with (a) $C = 1.8$ and (b) $C = 1.1$; the dotted curve shows the ECS fit to the $\Delta K = -3$ rates, as described in the text. Note that the estimated error on each rate parameter from the fit of the kinetic equation is approximately $\pm 20\%$.

C. Changes of J, $\Delta K = 0$, in NH_3–NH_3 and NH_3–Ar collisions

NH_3–NH_3. The detailed kinetic analysis provided rate constants and cross sections for J-changing collisions in which $\Delta K = 0$. Surprisingly, there are no simple dipolelike propensity rules. Although the largest cross sections were found for $\Delta J = 1$ transitions, there are also considerable amounts of $\Delta J = 2$ and 3 transitions. The rates for these processes could be scaled well by an EGL with $C = 1.8$ [Fig. 7(a)]. As expected, this is higher than for nonpolar molecules such as methane[13] ($C = 0.8$) or silane[60] ($C = 0.05$–0.08), but it is sufficiently low that "higher-order" transitions with $\Delta J = 2,3,...$ play a non-negligible role in the rotational relaxation in the different K stacks. We want to point out that the kinetic analysis unambiguously proves that these transitions are not equivalent to sequential dipolelike transitions with $\Delta J = 1$.

The first state-to-state collision data in the ground state of NH_3 were obtained by Oka *et al.*,[2] who performed microwave–microwave (MWMWDR) and IR–microwave double-resonance experiments yielding information on collision-induced transitions between two specific J_K inversion doublets. They found that the rotational relaxation of NH_3 in the ground state is governed by dipolelike propensity rules. Any "higher-order" transitions were found to be at least an order of magnitude slower than $\Delta J = 0$ or 1 transitions. In the $v_2 = 1$ state, however, nondipolar transitions make a significant contribution to the relaxation process.

NH_3–Ar. In the case of NH_3–Ar collisions, the propen-

sity rules are expected to be more complicated than in the NH_3–NH_3 case. Higher-order transitions with $\Delta J > 1$ are expected. The absolute rate constants for $\Delta J = 1$ transitions are considerably reduced compared to the self-relaxation in NH_3 and the individual rates follow the trend of the total depopulation rates [see Fig. 7(b)]. An EGL parameter $C = 1.1$, deduced from the kinetic model, shows that $\Delta J > 1$ transitions are relatively more probable than in the NH_3–NH_3 case. The qualitative picture here is in good agreement with the propensity rules derived by Oka from his microwave double-resonance studies.[2] In the recent experiments of Schliepen and ter Meulen,[12] they find large cross sections for $\Delta J > 1$ transitions (up to $\Delta J = 6$) in the ground state for NH_3–He at a collision energy of 54 meV. It is therefore quite reasonable that these transitions occur in the excited states of NH_3 in collisions with argon as well.

D. Changes of J, $\Delta K = 3$, in NH_3–NH_3 and NH_3–Ar collisions

NH_3–NH_3. From our kinetic model calculations we derived rate constants and cross sections for $\Delta J = 0, 1, \ldots, 4$ with $\Delta K = 3$ transitions for NH_3–NH_3 and NH_3–Ar collisions. The results are given in Table IV and Fig. 7(b). Direct evidence for the presence of these transitions is the early population of the $s(5,0)$ and especially the $s(1,0)$ states of NH_3. The rates for ΔJ–ΔK transitions decrease with increasing ΔJ (or energy gap) but not as fast as the pure J-changing collision rates with $\Delta K = 0$. They are always smaller than the corresponding pure J-changing rates. The results indicate that in a J-changing collision with a large J change it becomes more and more probable that K changes as well. These results do not agree with previous results of ground-state MWMWDR experiments in NH_3–NH_3, in which $\Delta K = 3$ transitions are at least 1 order of magnitude slower than $\Delta J = 0$ and 1. It is not entirely clear why this should be different in $v_2 = 1$. However, Kuze *et al.*[23] found in steady-state IR–IR double-resonance experiments a ratio of 2.5 between the rate for $\Delta J = 1$ and $\Delta K = 3$ transitions. This result agrees well with our observations. A possible explanation for the discrepancy of these experiments and Oka's might be that the effective rate for $\Delta K = 3$ transitions is nearly the same for the upper and the lower levels (whose population difference is monitored in MWMWDR) of an inversion doublet in the ground vibrational state if the $a \leftrightarrow s$ propensity rule does not hold for this process. The probability of $\Delta K = 3$ transitions seems to be larger at low temperatures. Surprisingly, Veeken, Dam, and Reuss[19] found that the $\Delta J = 1$, $\Delta K = 0$ ($J,K = 4,3 \rightarrow 3,3$) relaxation in the *ortho* species is not faster than the $\Delta K = 3$ transition ($J,K = 0,0 \rightarrow 3,3$) at low jet temperatures.

NH_3–Ar. Contrary to the self-relaxation results, $\Delta K = 3$ transitions have been expected and are observed for NH_3–Ar(rare-gas) collisions. In our case we derived rate constants and cross sections for $\Delta J = 0, 1, \ldots, 4$ transitions with $\Delta K = 3$ for NH_3–Ar collisions. As with NH_3–NH_3 collisions, the rates for ΔJ–ΔK transitions decrease with increasing ΔJ but not as much as the pure J-changing collision rates with $\Delta K = 0$.

The $\Delta K = 3$ collisional energy transfer that we have observed occurs with rates on the order of $1\ \mu s^{-1}\ Torr^{-1}$, corresponding to very small inelastic cross sections, on the order of 3.5 Å^2. The energy-corrected sudden (ECS) approximation[52,61,62] is applicable to systems in which the ratio of the collision duration to the rotational dephasing time is on the order of 1. For NH_3–NH_3 transitions between the 5,3 and 4,0 levels, this ratio is about 1, with the collision duration calculated as described in Ref. 61.

Since the collisional parameters for $\Delta K = 3$ are in an appropriate range, the ECS approximation should be applicable to these highly inelastic collisions. In this calculation, for such short-range collisions, we assume a high-order interaction with the potential having a high-n, r^{-n} dependence, and with the amplitudes spread over a wide range of tensor basis rate ranks, **L**, with little variation as a function of **L**. We estimated the collision duration from the observed cross sections for the 5,3 to 4,0 levels, giving $\tau_c \sim 0.1$ ps, and scaled the maximum of each curve to the $\Delta J = 0$ rate. As shown for NH_3–NH_3 in Fig. 7(a), and for NH_3–Ar in Fig. 7(b), the ECS approximation correctly predicts the scaling relationship between all of our observed 5,3 to J,0 rates. The slow falloff with J of the rates to $J < 5$ is qualitatively predicted by the ECS scaling law. For the transitions to $J > 5$, the ECS behavior is dominated by the detailed balance correction, and again qualitatively agrees with our experimental data. All of our observed $\Delta K = 3$ rates had been adjusted independently in the fit (Sec. IV C 2), without reference to the expected ECS behavior, so this result provides an unbiased verification of its predictions.[52]

E. Changes of parity in collisions

The effective rate of $a \leftrightarrow s$ transfer has been measured directly for the transition $s(6,1) \leftarrow a(6,1)$ after population of $a(6,1)$ with the $9R(30)$ line of the CO_2 laser. The kinetic model, with an average value of $k_{as} = 4\ \mu s^{-1}\ torr^{-1}$, fits the direct measurement very well, as can be seen from Fig. 3. Small variations of symmetry changing rates as a function of J and K have been neglected in the model.

Our value for k_{as} of about $4\ \mu s^{-1}\ torr^{-1}$ is lower than in the vibrational ground state [50–80 $\mu s^{-1}\ torr^{-1}$ (Refs. 18(b)–18(d), and 19], but is more than an order of magnitude higher than that recently reported by Shultz and Wei.[20] It is also higher than the $a \leftrightarrow s$ transfer in $v_2 = 2$ (approximately $2\ \mu s^{-1}\ torr^{-1}$),[22] although, in that case, the $a \leftrightarrow s$ transfer is probably a sequence of $a \leftrightarrow s$ and $\Delta J = 1$ transitions because the separations between the a and s levels is higher than the J,K spacing. Looking at the trend of this process in the v_2 progression, it is unlikely that the previously reported[20] value of $0.2\ \mu s^{-1}\ torr^{-1}$ can be correct.

Most striking, and against all dipolelike behavior, is the fact that we did not find a propensity rule for $a \leftrightarrow s$ processes in rotationally inelastic collisions. We could model the rotational energy transfer only if we relaxed this propensity rule. From our kinetic model we derived a ratio $\beta = k(a \leftrightarrow a)/k(a \leftrightarrow s) = k(s \leftrightarrow s)/k(a \leftrightarrow s) > 0.7$ for both self- and argon collisions. This means that there is no specific (a,s) correlation between states of opposite parity. In the case of ammonia self-relaxation, this is in sharp contrast to the results

inferred from the microwave double-resonance experiments.[2]

F. Collision rate and pressure-broadening coefficient

The total depopulation rates of the $s(5,3)$ level in $v_2 = 1$ and the ground-state recovery rate in $a(5,3)$ can be related to measurements of the pressure-broadening coefficients γ/p in the ammonia ν_2 infrared band[24-27] using the generally accepted relation[63,64]

$$\gamma/p(\text{MHz/torr}) = (1/2\pi)(k_u + k_l)/2;$$

that is, the broadening rate is the average of the inelastic collision rates k_u and k_l, expressed in $\mu s^{-1}\,\text{torr}^{-1}$, in the upper and lower levels of the spectroscopic transition. This relation assumes no contribution from inelastic dephasing or other non-state-changing processes.

For ammonia self-broadening, measurements[24-27] on rotational levels in the ν_2 fundamental comparable to those studied in this work yield values of 13.4 [for the $aR(0,0)$ line[27]] to 22 MHz/Torr, and 8–10 MHz/torr for the $2\nu_2-\nu_2$ hot-band lines. Use of our measured values for ground-state recovery and excited-state depopulation (Table II) in the preceding relation would predict broadening coefficients of about 9 MHz/torr, around 40% smaller than the experimental values. We believe that the explanation of this difference most consistent with existing data is a significant elastic contribution in the $v_2 = 1$ and $v_2 = 2$ levels to the linewidths, but not in the ground state. Our observed ground-state depopulation rate of $80\,\mu s^{-1}\,\text{torr}^{-1}$ is in close agreement with the microwave T_2/T_1 measurements of Schwendeman *et al.*[18(b)-18(d)] if a zero contribution from adiabatic processes is assumed, and our phenomenological rate is assumed to correspond to the rate of population transfer out of the combined inversion doublet pair. Schwendeman's measurements also indicate that, for high J levels, the sum of adiabatic processes and processes leaving the inversion doublet levels is less than 5% of the linewidth. Since the adiabatic contribution should depend only weakly on J, we infer a small contribution to low J levels from adiabatic collisions. Furthermore, a zero or very small adiabatic contribution in the ground state is in accord with Schwendeman's Anderson theory and sudden approximation calculations.[18(b)] Supporting Schwendeman's high J measurements, the line-mixing measurements of Henck and Lehmann[65] indicate that a large fraction of the linewidth for both $J = 4$ and $J = 8$ is due to the sum of elastic and inversion-doublet transitions. Even if k_l in the linewidth expression is set to the microwave value of 18.4 MHz/Torr (which would include any adiabatic contribution), the resulting values for γ are lower than the observed linewidths. This indicates that elastic processes make a significant contribution to relaxation in $v_2 = 1$ even though that contribution is negligible in $v_2 = 0$. A similar situation occurs in the $2\nu_2-\nu_2$ hot band, indicating adiabatic contributions in both $2\nu_2$ and ν_2. The triple-resonance measurements[22] yielded only a lower bound on the $v_2 = 2$ relaxation rate, $> 3\,\mu s^{-1}\,\text{torr}^{-1}$; if we assume that the relaxation rate in $v_2 = 2$ is the same as that in $v_2 = 1$, $34\,\mu s^{-1}\,\text{torr}^{-1}$, we can estimate an upper bound for the inelastic contribution to the $2\nu_2-\nu_2$ broadening rate of 5.4 MHz/torr.

For hydrogen-,[25] nitrogen-,[24] and argon-broadening,[24] the coefficients are ~3, 2.9–4.3, and 1.3–1.9 MHz/torr, respectively, for transitions between levels with J and K similar to those studied in this work. While we were able to obtain excited-state depopulation rates (see Table II), we did not obtain precise ground-state recovery rates for these gases as collision partners. Ground-state recovery rates about twice as large as the excited-state depopulation rates, as in ammonia self-collisions, would allow the foreign-gas linebroadening rates to be accounted for by the average of the inelastic collision rates in the upper and lower spectroscopic levels, in accordance with the standard model.[63,64]

A similar situation obtains for ozone, which has also been studied in our laboratory.[66] For that system, the self-broadening coefficient is about 20% larger than that which would be determined from upper- and lower-level relaxation rates measured by TRIRDR spectroscopy, while foreign-gas (nitrogen, oxygen) broadening can be accounted for in terms of these rates. In the case of d_4-methane, in which the inelastic collision rates are smaller than for polar species such as ozone or ammonia, the measured[67] self- and argon-Raman broadening coefficients are 30%–60% larger than the averaged relaxation rate.

These results can be understood if we interpret the discrepancies as contributions of elastic collision processes to the pressure-broadening coefficient. Since the time-resolved measurements probe the population difference of states, and thus the inelastic part of the collision process, while measurements in the frequency domain reflect the sum of all elastic and inelastic processes, it may be expected that the pressure-broadening coefficient will be greater than the corresponding inelastic collision rate whenever elastic processes are non-negligible. Recognition of this point may influence future theoretical calculations of pressure-broadening coefficients, which often neglect the elastic, or nonstate-changing, processes.[68] Analysis of the temperature dependence of the linewidths and relaxation rates would also be of interest, particularly in connection with remote sensing of the atmospheres of the outer planets.[9]

G. State-to-state rate constants and the intermolecular interaction potential

The rotational energy transfer of ammonia in self-collisions and collisions with rare-gas atoms, N_2 and H_2, has been the subject of many experimental and theoretical investigations in the past. One principal goal of these studies is the determination of the intermolecular potential of the collision partners.[11,69,70] It is obvious that this can only be done by the measurement of state-to-state rate constants and cross sections. Knowing the state-to-state inelastic cross sections or rate constants from experiment, it should be possible to construct the intermolecular potential by fitting the calculated cross sections to the experimental values. This "potential modeling" based on theoretical calculations will provide insight into the dynamics of the intermolecular collision process.

A detailed evaluation of the potential-energy surface parameters of the two collision partners (NH_3, Ar) is, in principle, possible[11] although not trivial for polyatomic collision

partners. Even without a detailed treatment it is possible to get a qualitative picture about the nature of the intermolecular forces by a careful examination of the cross sections for different processes and propensities obtained. In the following we try to explain the observed cross sections for ΔJ and ΔK and parity-changing collisions in terms of contributions of the different terms of the multipole expansion of the interaction potential.

One method for the description for the potential surface is the Hartree–Fock dispersion model (HFD).[11,69,70] In this model the interaction energy is partitioned into a Hartree–Fock energy contribution, obtained from accurate self-consistent-field calculations and a correlation energy contribution, which is in turn approximated by a damped multipolar dispersion expansion.[11,69,70] In the following section we want to discuss briefly which information can be obtained from state-resolved bulk experiments that can serve as first input data for the calculations mentioned above.

In our present investigations we extracted effective state-to-state rotational energy-transfer (RET) rates which can be converted into velocity-averaged cross sections (averaged over the thermal relative-velocity distribution). While the total depopulation cross sections are most sensitive to the total range of interaction (isotropic part of the interaction potential), the single state-to-state rates are sensitive to the anisotropic part of the potential as well. Different $\Delta J,\Delta K$ processes of NH_3 in collisions with NH_3 or Ar are correlated with different interaction forces and different "characters" of the collision process. The character of the collision process is sometimes expanded in an S matrix or tensor opacity decomposition which indicates the multipole nature of the collision-induced transitions, as is done in recent work on H_2CO.[71] The multiplicity of pathways in NH_3 $v_2 = 1$ relaxation makes it impossible to apply that method quantitatively.

In the following we want to examine the different cross sections obtained in the experiments and to correlate the cross sections and the multipole nature of the interaction potential. Since dipole, quadrupole, octopole, or higher-order multipole interactions have different ranges, and different induced transitions in the first Born approximation, the measurements of the different processes through observing different levels in $v_2 = 1$, probe different parts of the interaction potential.

Oka[2(f)] pointed out that, for a dipolar absorber, collision-induced transitions following $+ \leftrightarrow -$ and $\Delta J = 0,1$ ($\Delta K = 0$) are expected in first order. The "selection rules" $\Delta J = 0,1,2$ and $s(a) \leftrightarrow s(a)$ and $\Delta J = 0,1,2,3$, $s \leftrightarrow a$, $\Delta K = 0,3$ hold for quadrupole and octopole transitions, respectively. Expected propensities for a second-order dipole transition would be $\Delta J = 0,1,2$ and $s(a) \leftrightarrow s(a)$, $\Delta K = 0$. Generally, for an n-order process the "selection rule" would be $a(s) \leftrightarrow a(s)$ if n is even and $a \leftrightarrow s$ if n is odd and $\Delta J = 1,2,...n$, $\Delta K = 0$. Furthermore, according to Oka,[2(e)] a $(2^n\text{-pole})_1$–$(2^m\text{-pole})_2$ interaction gives $a(s) \leftrightarrow a(s)$ transitions for even n and $s \leftrightarrow a$ transitions for odd n in molecule 1. A $(2^n\text{-pole})_1$–$(2^m\text{-pole induced dipole})_2$ interaction causes $a(s) \leftrightarrow a(s)$ for even $n + m$ and $s \leftrightarrow a$ transitions for odd $m + n$.

We believe that the rather unsystematic parity selection rule in NH_3–NH_3 and NH_3–Ar collisions obtained in our experiments cannot be explained by any single interaction mentioned above. In the case of NH_3–NH_3 collisions the leading term in the multipole expansion is certainly the dipole term. The cross sections obtained for $s \leftrightarrow a$ and $\Delta J = 0,1$ are the largest. This was verified by a direct measurement of the $s(6,1)$ and $s(5,1)$ levels for $a(6,1)$ excitation ($9R$ 30). On the other hand, we derive from direct measurements of the $s(4,3)$ and $s(6,3)$ with $s(5,3)$ excitation ($10P$ 32) that $s \leftrightarrow s$ transitions in the case of $\Delta J = 1$ are fast as well. Without a fast tunneling process during the collision duration,[12] these transitions can be regarded as quadrupolar transitions with probabilities, according to the cross sections we obtained, on the same order as the dipolar transitions. Similarly, for $\Delta J = 2$, $\Delta K = 0$, transitions, the probability for $s(a) \leftrightarrow s(a)$ and $s \leftrightarrow a$ transitions are almost the same. The $s(a) \leftrightarrow s(a)$ transitions correspond most closely to a high-order dipole or a quadrupole transition (or the dispersion interaction of r^{-6}) and the $s \leftrightarrow a$ to an octopolar transition. In case of $\Delta J = 3$, $\Delta K = 0$, the different $a(s) \leftrightarrow a(s)$ and $s \leftrightarrow a$ transitions can be regarded as higher-order dipole, or octopole or higher multipole interactions. These multipolar arguments apply only to transitions in the same "K stack." For $\Delta J,\Delta K$ transitions, octopolar interactions, a vibrational-mixing-induced dipole[72–74] ($\Delta J = 0,1$ only), or the dispersion interaction of r^{-7}, are necessary to account for a change of K by 3 and simultaneous change in J. In the case of NH_3–Ar collisions, similar arguments are possible in terms of $(2^n\text{-pole})_1$–$(2^m\text{-pole induced dipole})_2$ interactions.

In summary, we want to point out that by probing different states in the $K = 0$ ($\Delta K = -3$) and $K = 3$ ($\Delta K = 0$) "stacks" in $v_2 = 1$ we are able to probe the short-range and long-range parts of the interaction potential. We are of course aware of the problems of converting the data obtained into potential surface parameters, but it seems to be clear that higher terms in the multipole expansion play a considerable role in the RET behavior of NH_3 in collisions with other molecules. Therefore one has to consider carefully where to truncate the expansion terms in the interaction potential expression in a calculation of NH_3 RET cross sections.

Our conclusion is that the rotational relaxation of NH_3 by NH_3 and by Ar have significant contributions from "hard" collisions. During a collision the molecules approach sufficiently close that the interaction is strong enough to cause the nondipolar transitions that we unambiguously observed. In these collisions, information about the initial state (J,K parity) is almost completely lost.

This behavior in $v_2 = 1$ is in contrast to the collision behavior in the vibrational ground state where dipolar $a \leftrightarrow s$ and $\Delta J = 1$ transitions dominate rotational energy transfer. In this case the collisions are "soft" collisions. Parity-changing [$s(a) \leftrightarrow a(s)$] transitions can be induced by the smallest long-range perturbation due to the small energy gap of the inversion doublets.

The information about the real "nature" of the collision process between NH_3 and NH_3(Ar) in $v_2 = 1$ can at this point only be qualitative; however, our results show that the interactions in both NH_3–NH_3 and NH_3–Ar collisions are

not due to one single multipole or multipole–(induced multipole) interaction and that rotational energy transfer is not governed by simple dipolar "selection rules." The obtained cross sections are, in any case, a critical test and a benchmark for any quantum-dynamical calculation.

ACKNOWLEDGMENTS

This work was supported by NASA Office of Space Science and Applications Upper Atmosphere Research Program Grant No. NAGW-1667 and Planetary Atmospheres Program Grant No. NAGW-2387, and by NSF Grant No. CHE89-14953 to the G. R. Harrison Spectroscopy Laboratory. B.A. has been supported by a fellowship from the Deutsche Forschungsgemeinschaft. S.L.C. has been supported by the Donors to Petroleum Research Fund, administered by the American Chemical Society. We thank Dr. G. Millot and M. G. Fanjoux of the Laboratoire de Spectronomie Moleculaire, Universite de Bourgogne, Dijon, France, for carrying out a fit of the exponential-gap scaling law similar to that shown in Fig. 5, and for cordial discussions. We dedicate this paper to Professor Takeshi Oka on the occasion of his 60th birthday and thank him for insightful comments on the paper.

[1] For reviews of early work on this system, see J. I. Steinfeld and P. L. Houston, in *Laser and Coherence Spectroscopy*, edited by J. I. Steinfeld (Plenum, New York, 1978), pp. 1–123; T. G. Schmalz and W. H. Flygare, *ibid.*, pp. 125–196.

[2] (a) T. Oka, J. Chem. Phys. **45**, 754 (1966); (b) **47**, 13, 4852 (1967); (c) **48**, 4919 (1968); (d) **49**, 3135 (1968); (e) P. W. Daly and T. Oka, *ibid.* **53**, 3272 (1970); (f) T. Oka, Adv. At. Mol. Phys. **9**, 12, (1973); (g) A. R. Fabris and T. Oka, J. Chem. Phys. **56**, 3168 (1972); (h) T. Oka, in *Interstellar Molecules*, edited by B. H. Andrews (IAU, 1980), p. 221; (i) A. R. Fabris and T. Oka, J. Chem. Phys. **78**, 3462 (1983).

[3] (a) J. M. Levy, J. H.-S. Wang, S. G. Kukolich, and J. I. Steinfeld, Phys. Rev. Lett. **29**, 395 (1972); (b) J. H.-S. Wang, J. M. Levy, S. G. Kukolich, and J. I. Steinfeld, Chem. Phys. **1**, 141 (1972); (c) G. M. Dobbs, R. H. Micheels, J. I. Steinfeld, J. H.-S. Wang, and J. M. Levy, J. Chem. Phys. **63**, 1904 (1975).

[4] (a) T. Shimizu and T. Oka, J. Chem. Phys. **53**, 2536 (1970); (b) T. Shimizu and T. Oka, Phys. Rev. A **2**, 1177 (1970).

[5] J. M. Levy, J. H.-S. Wang, S. G. Kukolich, and J. I. Steinfeld, Chem. Phys. Lett. **21**, 598 (1973).

[6] A. Das and C. H. Townes, J. Chem. Phys. **85**, 179 (1986).

[7] S. Kano, T. Amano, and T. Shimizu, Chem. Phys. Lett. **25**, 119 (1974).

[8] J. A. Silver, D. S. Bomse, and A. C. Stanton, Appl. Opt. **30**, 1505 (1991).

[9] Proceedings of the Conference on Laboratory Research for Planetary Atmospheres, Bowie, Maryland, 1989, edited by T. R. Spilker and V. R. Eshleman (unpublished); P. Varanasi, J. Quantum Spectrosc. Radiat. Transfer **39**, 13 (1988).

[10] D. B. M. Klaassen, J. M. H. Reijnders, J. J. ter Meulen, and A. Dymanus, J. Chem. Phys. **76**, 3019 (1982); D. B. M. Klaassen, J. J. ter Meulen, and A. Dymanus, *ibid.* **77**, 4972 (1982); **78**, 767 (1983).

[11] G. Ebel, R. Krohne, H. Meyer, U. Buck, R. Schinke, T. Seeleman, P. Andresen, J. Schliepen, J. J. ter Meulen, and G. H. F. Diercksen, J. Chem. Phys. **93**, 6419 (1990); H. Meyer, U. Buck, R. Schinke, and G. H. F. Diercksen, *ibid.* **84**, 4976 (1986).

[12] J. Schliepen and J. J. ter Meulen (unpublished).

[13] B. Foy, J. Hetzler, G. Millot, and J. I. Steinfeld, J. Chem. Phys. **88**, 6838 (1988).

[14] J. R. Hetzler and J. I. Steinfeld, J. Chem. Phys. **92**, 7135 (1990).

[15] C. Flannery, Y. Mizugai, J. I. Steinfeld, and M. N. Spencer, J. Chem. Phys. **92**, 5164 (1990).

[16] D. J. Danagher and J. Reid, J. Chem. Phys. **86**, 5449 (1987).

[17] P. Dube and J. Reid, J. Chem. Phys. **90**, 2892 (1989).

[18] (a) Y. Matsuo, S. K. Lee, and R. H. Schwendeman, J. Chem. Phys. **91**, 3948 (1989); (b) K. L. Peterson and R. H. Schwendeman, *ibid.* **75**, 5662 (1981); (c) T. Amano, T. Amano, and R. H. Schwendeman, *ibid.* **73**, 1238 (1980); (d) T. Amano and R. H. Schwendeman, *ibid.* **65**, 5133 (1976).

[19] K. Veeken, N. Dam, and J. Reuss, Chem. Phys. **100**, 171 (1985).

[20] M. J. Shultz and J. Wei, J. Chem. Phys. **92**, 5951 (1990).

[21] T. Seelemann, P. Andresen, and E. W. Rothe, Chem. Phys. Lett. **146**, 82 (1988).

[22] B. Abel, J. J. Klaassen, S. L. Coy, and J. I. Steinfeld, Spectrochim. Acta **47A**, 973 (1991).

[23] H. Kuze, H. Jones, M. Tsukakoshi, A. Minoh, and M. Takami, J. Chem. Phys. **80**, 4222 (1984).

[24] D. H. Beckwith, D. J. Danagher, and J. Reid, J. Mol. Spectrosc. **121**, 209 (1987).

[25] J. S. Margolis and S. Sarangi, J. Quantum Spectrosc. Radiat. Transfer **16**, 405 (1976).

[26] (a) G. Baldacchini, S. Marchetti, V. Montelatici, G. Buffa, and O. Tarrini, J. Chem. Phys. **76**, 5271 (1982); (b) G. Baldacchini, A. Bizzarri, L. Nencini, G. Buffa, and O. Tarrini, J. Quantum Spectrosc. Radiat. Transfer **42**, 423 (1989).

[27] T. Shimizu, F. O. Shimizu, R. Turner, and T. Oka, J. Chem. Phys. **55**, 2822 (1971).

[28] C. Flannery, J. J. Klaassen, M. Gojer, J. I. Steinfeld, M. Spencer, and C. Chackerian, Jr., J. Quantum Spectrosc. Radiat. Transfer **46**, 73 (1991).

[29] G. Guelachvili and K. N. Rao, *Handbook of Infrared Standards* (Academic, New York, 1986).

[30] H. Jones, Appl. Phys. **15**, 261 (1978).

[31] M. Fourrier and M. Redon, Appl. Phys. Lett. **21**, 463 (1972); M. Redon, H. Gurel, and M. Fourrier, Chem. Phys. Lett. **30**, 99 (1975).

[32] S. M. Freund and T. Oka, Appl. Phys. Lett. **21**, 60 (1972).

[33] R. V. Ambartzumyan, V. S. Letokhov, G. N. Makarov, and A. A. Puretzkii, JETP Lett. **15**, 501 (1972); **17**, 63 (1973).

[34] Ph. Avouris, M. M. T. Loy, and I. Y. Chan, Chem. Phys. Lett. **63**, 624 (1979).

[35] J. D. Campbell, G. Hancock, J. B. Halpern, and K. H. Welge, Chem. Phys. Lett. **44**, 404 (1976).

[36] Yu. A. Kuritsyn, G. N. Makarov, V. R. Mironenko, and I. Pak, Opt. Spektrosk. (USSR) **69**, 543 (1990).

[37] J. Eggleston, J. Dallarossa, W. K. Bischel, J. Bokor, and C. K. Rhodes, J. Appl. Phys. **50**, 3867 (1979).

[38] H. D. Morrison, J. Reid, and B. K. Garside, Appl. Phys. Lett. **45**, 321 (1984).

[39] A. N. Bobrovskii, A. A. Vedenov, A. V. Kozhevnikov, and D. N. Soblenko, JETP Lett. **29**, 536 (1979).

[40] P. Pinson, A. Delage, G. Girard, and M. Michon, J. Appl. Phys. **52**, 2634 (1981).

[41] S. Urban, D. Papousek, J. Kauppinen, K. Yamada, and G. Winnewisser, J. Mol. Spectrosc. **101**, 1 (1983).

[42] S. Urban, R. D'Cunha, K. N. Rao, and D. Papousek, Can. J. Phys. **62**, 1775 (1984).

[43] S. Urban, V. Spirko, D. Papousek, R. S. McDowell, N. G. Nereson, S. P. Belov, L. I. Gershstein, A. V. Maslovskij, A. F. Krupnov, J. Curtis, and K. N. Rao, J. Mol. Spectrosc. **79**, 455 (1980).

[44] H. O. Everett and F. C. De Lucia, J. Chem. Phys. **92**, 6480 (1990).

[45] F. Menard-Bourcin and L. Doyennette, J. Chem. Phys. **88**, 5506 (1988).

[46] I. Oppenheim, K. E. Shuler, and G. H. Weiss, Adv. Mol. Relaxation Processes **1**, 13 (1967–68).

[47] I. Oppenheim, K. E. Shuler, and G. H. Weiss, *Stochastic Processes in Physical Chemistry: The Master Equation* (MIT, Cambridge, MA, 1977).

[48] J. I. Steinfeld, J. S. Francisco, and W. L. Hase, *Chemical Kinetics and Dynamics* (Prentice-Hall, Englewood Cliffs, NJ, 1989), pp. 474–488.

[49] B. J. Orr, Int. Rev. Phys. Chem. **9**, 67 (1990).

[50] T. Brunner and D. Pritchard, Adv. Chem. Phys. **50**, 589 (1982).

[51] A. J. McCaffery, M. J. Proctor, and B. J. Whitaker, Annu. Rev. Phys. Chem. **37**, 223 (1986).

[52] J. I. Steinfeld, P. Ruttenberg, G. Millot, G. Fanjoux, and B. Lavorel, J. Phys. Chem. **95**, 9638 (1991).

[53] W. H. Press, B. P. Flannery, S. A. Teukolsky, and W. T. Vetterling, *Numerical Recipes* (*FORTRAN*) (Cambridge University, Cambridge, 1985).

[54] D. Harradine, B. Foy, L. Laux, M. Dubs, and J. I. Steinfeld, J. Chem. Phys. **81**, 4267 (1984).

[55] J. J. Klaassen and B. Abel (unpublished).

[56] C. C. Jensen, T. G. Anderson, C. Reiser, and J. I. Steinfeld, J. Chem.

Phys. **71**, 3648 (1979); M. Dubs, D. Harradine, E. Schweitzer, and J. I. Steinfeld, *ibid.* **77**, 4267 (1984).
[57] F. Temps, S. Halle, P. H. Vaccaro, R. W. Field, and J. L. Kinsey, J. Chem. Soc. Faraday Trans. 2 **84**, 1457 (1988).
[58] *Atom-Molecule Collision Theory: A Guide for the Experimentalist*, edited by R. B. Bernstein (Plenum, New York, 1979), pp. 259–375.
[59] I. Procaccia and R. D. Levine, J. Chem. Phys. **63**, 4261 (1975); M. Rubinson and J. I. Steinfeld, Chem. Phys. **4**, 167 (1975).
[60] J. R. Hetzler and J. I. Steinfeld, J. Chem. Phys. **92**, 7135 (1990).
[61] A. E. DePristo, A. D. Augustin, R. Ramaswamy, and H. Rabitz, J. Chem. Phys. **74**, 5037 (1981).
[62] T. A. Brunner, N. Smith, A. W. Karp, and D. E. Pritchard, J. Chem. Phys. **74**, 3324 (1981).
[63] A. E. DePristo and H. Rabitz, J. Chem. Phys. **69**, 902 (1978).
[64] A. E. DePristo and H. Rabitz, J. Quantum Spectrosc. Radiat. Transfer **22**, 65 (1979).
[65] S. Henck and K. K. Lehmann, Chem. Phys. Lett. **144**, 281 (1988).
[66] C. C. Flannery and J. I. Steinfeld, J. Chem. Phys. (in press).
[67] G. Millot, B. Lavorel, and J. I. Steinfeld, J. Quantum Spectrosc. Radiat. Transfer (in press).
[68] A. Levy, N. Lacome, and C. Chackerian, Jr., in *Spectroscopy of the Earth's Atmosphere and Interstellar Molecules*, edited by K. N. Rao and A. Weber (Academic, New York, in press), and references therein.
[69] C. Douketis, J. M. Hutson, B. J. Orr, and G. Scoles, Mol. Phys. **52**, 763 (1984).
[70] R. Alrichs, R. Penco, and G. Scoles, Chem. Phys. **19**, 119 (1979).
[71] S. L. Coy, S. Halle, J. L. Kinsey, and R. W. Field, J. Mol. Spectrosc. (in press).
[72] T. Oka, F. O. Shimizu, T. Shimizu, and J. K. G. Watson, Astrophys. J. **165**, L15-19.
[73] T. Oka, in *Molecular Spectroscopy: Modern Research, Vol. II* (Academic, New York, 1976), p. 229.
[74] D. Laughton, S. M. Freund, and T. Oka, J. Mol. Spectrosc. **62**, 263 (1976).